Available online at www.sciencedirect.com
SCIENCE DIRECT®
Solid State Communications 130 (2004) 429–432
solid state communications
www.elsevier.com/locate/ssc

Autocatalytic redox fabrication and magnetic studies of Co–Ni–P alloy nanowire arrays

X.Y. Yuan[a,b,*], G.S. Wu[a], T. Xie[a], Y. Lin[a], G.W. Meng[a], L.D. Zhang[a]

[a]*Nanometer Group, Institute of Solid State Physics, Chinese Academy of Sciences, P.O. Box 1129, Hefei, Anhui Province, 230031, People's Republic of China*
[b]*Department of Chemistry, Anhui University, Hefei 230039, People's Republic of China*

Received 12 November 2003; received in revised form 15 December 2003; accepted 17 December 2003 by C.E.T. Gonçalves da Silva

Abstract

Uniform and large-scale Co–Ni–P alloy nanowire arrays have been fabricated by autocatalytic redox reaction in an anodic alumina membrane (AAM). The images of Co–Ni–P alloy nanowire arrays and single nanowires are obtained by scanning electron microscope (SEM) and transmission electron microscope (TEM), respectively. Selected area electron diffraction (SAED), X-ray diffraction (XRD) and energy dispersive spectra (EDS) are employed to study the morphology and chemical composition of the nanowires. The results indicate that the Co–Ni–P nanowire arrays are amorphous in structure. The magnetic property of Co–Ni–P nanowire arrays is characterized using a vibrating sample magnetometer (VSM). The hysteresis loops show that the easily magnetized direction of Co–Ni–P nanowire arrays is parallel to the nanowire arrays and that it has obvious magnetic anisotropy as a result of the shape anisotropy.

PACS: 81.16.Be; 75.30.Gw; 75.75. + a; 81.16. − c

Keywords: A. Magnetically ordered materials; A. Nanostructures; B. Chemical synthesis; B. Nanofabrications; C. Scanning and transmission electron microscopy

1. Introduction

In recent years, fabrication of nanowire arrays, especially magnetic nanowire arrays, has become the subject of intensive study [1–4] due to their potential applications in the ultra-high-density magnetic storage devices and microsensors [5]. Magnetic nanowire arrays as an ultra-high-density magnetic storage material can achieve recoding densities of more than 100 Gbit/in^2, which is beyond the projected thermal limits of 40 Gbit/in^2 in continuous magnetic film [6,7]. This kind of usage mainly takes advantage of the perpendicular anisotropy as a result of the shape anisotropy of nanowire arrays. But in some cases (such as Co, Ni nanowires), due to the competition between magnetocrystalline anisotropy and shape anisotropy, there may be no perpendicular anisotropy [8,9]. Since the magnetic properties of nanowire arrays are related to their element components and morphology, ternary alloy amorphous magnetic nanowire arrays are expected to exhibit the perpendicular anisotropy. An aim to be pursued is to fabricate perpendicular anisotropy ternary magnetic nanowire arrays for ultra-high-density magnetic recording. Although there have been reports of fabrication of single-element and binary alloy magnetic nanowire arrays by electrodeposition in anodic alumina membrane (AAM) [10–13], ternary alloy magnetic nanowire arrays have not been reported so far. Because the redox evolution potential and thermodynamic stability of these elements are different, it is very difficult to electrodeposit large-scale and uniform ternary alloy nanowire arrays in an aqueous solution, especially in a

* Corresponding author. Address: Nanometer Group, Institute of Solid State Physics, Chinese Academy of Sciences, P.O. Box 1129, Hefei, Anhui Province, 230031, People's Republic of China. Tel./fax: + 86-551-559-1434.
E-mail address: hfyxy@sohu.com (X.Y. Yuan).

0038-1098/$ - see front matter © 2003 Elsevier Ltd. All rights reserved.
doi:10.1016/j.ssc.2003.12.028

solution containing such element as phosphor (P). In addition, there are also some defects in electrodeposition method, just as Prieto described [14], several factors affect the degree of pores filling in AAM. First, pore-to-pore variations in nucleation rate arise from the presence of heterogeneities at the cathode interface, such as grain boundaries or adsorbed impurities. Second, even if wires are nucleated in all the pores, the rate of growth must be uniform so that all wires grow to the length of the pore simultaneously. If a few pores fill rapidly, then growth continues laterally across the top surface, closing off unfilled pores in the process. Third, if there are very small cracks in the AAM, even slightly larger than the pore diameter, deposition will occur predominantly in the cracks owing to point discharge and uneven current distribution in the pores of AAM. Here, we have succeeded in fabricating uniform size and shape of Co–Ni–P nanowire arrays on a large-scale by autocatalytic redox reaction in AAM. Compared with electrodeposition method, autocatalytic redox method needs neither a supply of power nor a sprinkling of gold (Au, as a conductive layer) on one side of the AAM before the deposition, which is carried out via the redox reaction of an oxidizer and a reductant in an electrolyte solution. It is an autocatalytic self-assembly process which is promising for the production of uniform nanowire arrays on a large-scale, and more importantly it will make it possible to finely control the aspect ratio of the nanowire using pores of different diameters and AAM thicknesses. Control of the uniform size and shape of nanowire arrays on a large-scale is recognized as a very important issue in the fabrication of nanostructure and turned out to be a challenging problem [15–18]. In addition, the autocatalytic redox method can be applied to many other materials [1] and open up significant opportunities in the nanoscale fabrication of magnetic materials for ultra-high-density magnetic recoding.

2. Experimental

The AAM template was prepared just as described in Masuda and Fukuda [19]. The pores of the AAM template are about 70 nm in diameter and 10 μm in length with interpores spacing of 100 nm. The though-hole AAM template was first immersed in an aqueous solution of $SnCl_2$ (10 g l^{-1}) for 1 min. and washed with distilled water 2 ~ 3 times, and then, the AAM template was further kept in a solution of $PdCl_2$ (1 g l^{-1}) for 30 s and rinsed with distilled water several times again. Subsequently, Co–Ni–P nanowire arrays were deposited in the pores of the AAM from a solution of 15 g l^{-1} $CoSO_4{\cdot}7H_2O$, 8 g l^{-1} $NiSO_4{\cdot}6H_2O$, 22 g l^{-1} $NaH_2PO_2{\cdot}H_2O$ and 60 g l^{-1} Rochelle salt at 80–85 °C.

In order to isolate the Co–Ni–P nanowire arrays, the AAM with Co–Ni–P nanowire arrays was dissolved in 5 wt% NaOH solution at 25 °C for 5 min and slightly washed several times with distilled water to remove the dissolved AAM and the remaining NaOH solution. For the scanning electron microscope (SEM, JSM-6700F) images, the above Co–Ni–P nanowire arrays were directly mounted on Cu stubs with a conductive gold paint. The sample for the transmission electron microscope (TEM, H-800) was treated with a 5 wt% NaOH solution for 10 min and dispersed in alcohol. Then a small drop of the solution was placed on a carbon film supported by Cu grids.

Selected area electron diffraction (SAED), energy dispersive spectra (EDS, TEM JEOL-2010) and X-ray diffraction (XRD, MXP18AHF) were employed to study the chemical composition and morphology of the nanowires. The magnetic property of Co–Ni–P alloy nanowire arrays was characterized using a vibrating sample magnetometer (VSM, BHV-55), with the applied magnetic field parallel or perpendicular to nanowire arrays.

3. Results and discussion

Fig. 1 shows a SEM image of Co–Ni–P alloy nanowire arrays prepared by autocatalytic redox reaction in an AAM. Fig. 1(a) is a top view image, Fig. 1(b) is a side view image and Fig. 1(c) is a SEM image of Co–Ni–P deposited in the pores wall (see bright dots) of AAM for 20 second. We know from Fig. (1) that Co–Ni–P nanowires are grown out from the pores of AAM. Therefore, the Co–Ni–P nanowire is about 70 nm in diameter, which is consistent with the pore diameter of the AAM. The autocatalytic redox reactions of Co–Ni–P nanowire arrays are as follows:

$$SnCl_2 + PdCl_2 = SnCl_4 + Pd \tag{1}$$

$$Ni^{2+} + 2e = Ni \qquad E^O = -0.25\ V \tag{2}$$

$$Co^{2+} + 2e = Co \qquad E^O = -0.28\ V \tag{3}$$

$$H_2PO_2^- + H_2O = H_2PO_3^- + 2H^+ + 2e \qquad E^O = -0.50\ V \tag{4}$$

$$H_2PO_2^- + 2H^+ + e = P + 2H_2O \qquad E^O = -0.25\ V \tag{5}$$

The E^O represents standard single electrode potential. If the E^O value of a reductant is lower than that of an oxidizer, the reaction between an oxidizer and a reductant will be possible to take place in the view of thermodynamics. The larger the electrode potential difference between an oxidizer and a reductant is, the higher the possibility of redox reaction is. According to the E^O values, Co, Ni and P could be reduced by NaH_2PO_2 in electrolyte solution. However, these reactions among (2), (3), (4) and (5) cannot take place without some catalyst, which is controlled by kinetics. Pd atoms act as a catalyst in the reactions. The growth mechanism of Co–Ni–P nanowire arrays may be described as follows: first, $SnCl_2$ solution which is adhered to the pore wall of the AAM hydrolyzes formation $Sn(OH)_2$ in an aqueous solution, then, $PdCl_2$ is reduced to Pd atoms by

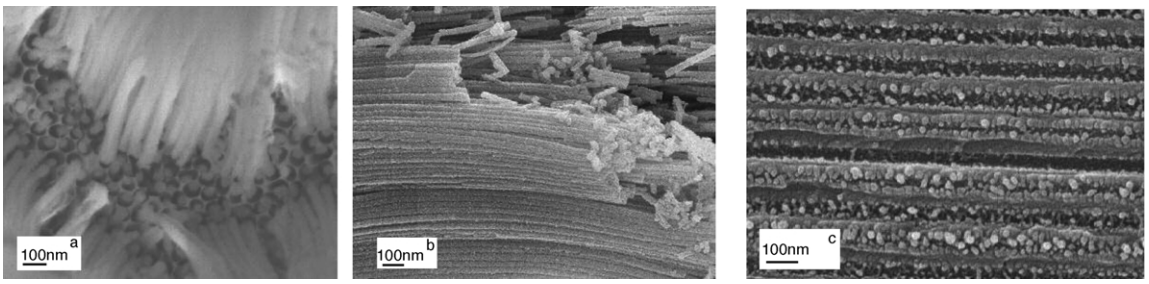

Fig. 1. SEM images of Co–Ni–P nanowire arrays, (a) top view image, (b) side view image, (c) Co–Ni–P deposited in the pores wall (see bright dots) of AAM for 20 s.

$Sn(OH)_2$. Consequentially, these Pd atoms trigger the redox reactions. Once the redox reactions are triggered, the above reactions of (2), (3), (4) and (5) can be autocatalyzed. In fact, as a catalyst, the concentration of Pd atoms is very low so that no trace of it is seen on the EDS spectrum in Fig. 3. Since autocatalytic redox reaction needs neither a supply of power nor a sprinkling of Au on one side of the AAM in the fabrication process of Co–Ni–P nanowire arrays, and since these redox reactions are autocatalytic self-assembly process and the electrolyte solution concentration is uniform, Co–Ni–P nanowire arrays are formed where there is the electrolyte solution, the Co–Ni–P nanowire arrays are definitely going to be uniform in size and shape on a large-scale (see Fig. 1 SEM images), and all wires grow to the same length in the pore simultaneously, as before some electrodeposition defects can be overcome. The TEM and SAED images of single Co–Ni–P nanowire are shown in Fig. 2. Fig. 2(a) indicate that the Co–Ni–P nanowire is about 70 nm in diameter and 3 μm in length. Fig. 2(b) shows that Co–Ni–P nanowire is amorphous in structure, which is confirmed by the XRD spectrum as shown in Fig. 3. This amorphous structure of Co–Ni–P nanowire arrays will meet the need of perpendicular anisotropy in magnetic properties. The EDS spectrum reveals that the nanowires are composed of Co, Ni and P, the atomic ratio is 42.82:40.48:16.70 and the mass ratio is 46.58:43.87:9.55.

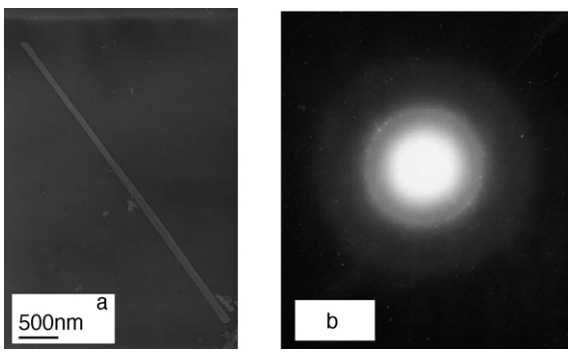

Fig. 2. (a) TEM image of Co–Ni–P alloy nanowire with diameter about 70 nm. (b) SAED of Co–Ni–P alloy nanowire.

Fig. 4 is the hysteresis loop of Co–Ni–P nanowire arrays measured at room temperature. The H ⊥ represents external magnetic field parallel to the Co–Ni–P nanowire arrays and the H‖ represents external magnetic field perpendicular to the Co–Ni–P nanowire arrays. As can be seen, the values of saturation magnetization (M_s) and remanence (M_r) of H ⊥ are both larger than those of H‖. The coercivities (Hc) of Co–Ni–P nanowire arrays for H ⊥ and H‖ orientation are about 750 and 800 Oe, respectively. Compared with the Hc (1200 Oe) of Co–P nanowire arrays [1], the Co–Ni–P nanowire arrays is much more suitable to magnetic recoding. In fact, the values of coercivity and saturation magnetization are under influence of many factors, such as the aspect ratio of Co–Ni–P nanowire and the element content of Co–Ni–P nanowire, the above results are only an average of the Co–Ni–P nanowire arrays. If the magnetic properties of single nanowire can be measured, it will be an interesting thing. The hysteresis loops indicate that the easily magnetized direction of Co–Ni–P nanowire arrays is parallel to the nanowire arrays and that it has obvious magnetic anisotropy. We can expect from the images of SAED and XRD that the competition between shape anisotropy and magnetocrystalline anisotropy is unlikely to occur in the present case, because this latter contribution doesn't exist due to the amorphous structure of these Co–Ni–P nanowires. The magnetic anisotropy of Co–Ni–P nanowires is a result of the shape anisotropies. It is due to the perpendicular anisotropy that the Co–Ni–P nanowire arrays are a candidate for ultra-high-density magnetic recoding media. The subject is therefore of interest in the field of magnetic nanostructures preparation and their associated anisotropy properties.

4. Conclusion

Uniform size and shape of Co–Ni–P magnetic nanowire arrays have been successfully fabricated on a large-scale by autocatalytic redox method in AAM. The results indicate that the Co–Ni–P nanowire arrays are amorphous in structure. The hysteresis loops show that the easily

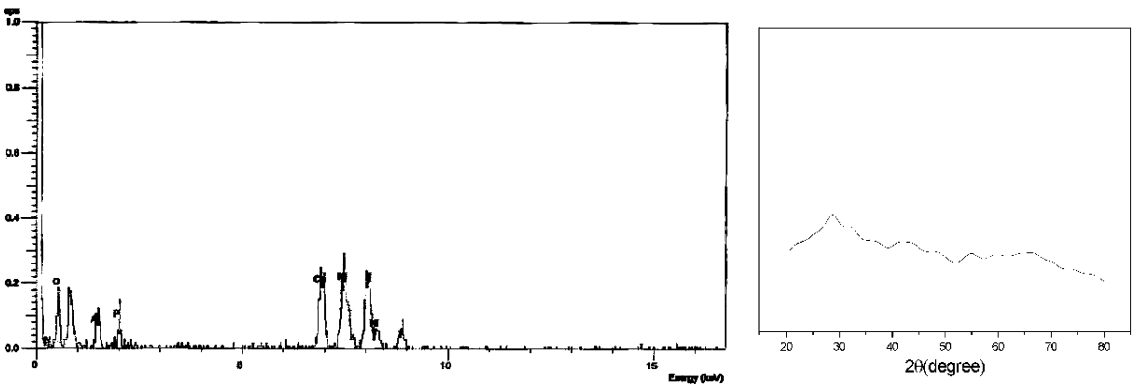

Fig. 3. The EDS (left) and XRD (right) of Co–Ni–P alloy nanowire. The EDS show the atomic ration and the mass ration of Co–Ni–P nanowire are 42.82:40.48:16.70, 46.58:43.87:9.55, respectively. The unlabelled peaks associated with copper coming from the TEM grid.

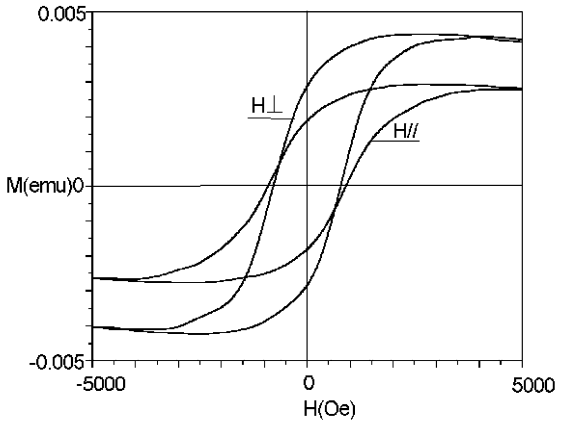

Fig. 4. Hysteresis loops of Co–Ni–P nanowire arrays embedded in AAM at room temperature. The H ⊥ represents magnetic field applied parallel to Co–Ni–P nanowire arrays and the H|| represents magnetic field applied perpendicular to Co–Ni–P nanowire arrays.

magnetized direction of Co–Ni–P nanowire arrays is parallel to the nanowire arrays and that it has obvious magnetic anisotropy as a result of the shape anisotropy. Autocatalytic redox method can be applied to many other materials and opens up significant opportunities in the nanoscale fabrication of magnetic materials for ultra-high-density magnetic recoding.

Acknowledgements

This work was supported by the Ministry of Science and Technology of China (Grant No.1999064501) and the National Science Foundation of China (Grant No. 10074064).

References

[1] X.Y. Yuan, G.S. Wu, T. Xie, Y. Lin, L.D. Zhang, Nanotechnology 15 (2004) 59.
[2] M. Shima, M. Hwang, C.A. Ross, J. App. Phys. 93 (2003) 3440.
[3] C.A. Ross, M. Hwang, M. Shima, H.I. Smish, M. Farhoud, T.A. Savas, W. Schwarzacher, J. Parrochon, W. Escoffier, H. Neal Bertram, F.B. Humphrey, M. Redjdal, J. Magn. Magn. Mater. 249 (2002) 200.
[4] A.J. Bennett, J.M. Xu, Appl. Phys. Lett. 82 (2003) 3304.
[5] S. Sun, C.B. Murray, D. Weller, L. Folks, A. Moser, Science 287 (2000) 1989.
[6] D. Routkevitch, A.A. Tager, J. Haruyama, D. Almawlawi, M. Moskovits, J.M. Xu, IEEE Trans. Electron Devices 43 (1996) 1646.
[7] P.L. Lu, S.H. Charap, IEEE Trans. Magn. 30 (1994) 4230.
[8] L. Piraux, S. Dubois, E. Ferain, J. Magn. Magn. Mater. 165 (1997) 352.
[9] P.M. Paulus, F. Luis, M. Kröll, G. Schmid, L.J. de Jongh, J. Magn. Magn. Mater. 224 (2001) 180.
[10] W. Chen, S.L. Tang, M. Lu, Y.W. Du, J. Phys.: Condens. Matter 15 (2003) 4623.
[11] A.J. Yin, J. Li, W. Jian, A.J. Bennett, J.M. Xu, Appl. Phys. Lett. 79 (2001) 1039.
[12] S. Park, S. Kim, S. Lee, Z.G. Khim, K. Char, T. Hyeon, J. Am. Chem. Soc. 22 (2000) 8581.
[13] Y.W. Wang, G.W. Meng, C.H. Ling, G.Z. Wang, L.D. Zhang, Chem. Phys. Lett. 343 (2001) 174.
[14] A.L. Prieto, M.S. Sander, M.S. Martin, R. Gronsky, T. Sands, A.M. Stacy, J. Am. Chem. Soc. 123 (2001) 7160.
[15] C.P. Gibson, K.J. Putzer, Science 267 (1995) 1338.
[16] M.P. Pileni, B.W. Ninham, T.G. Krzywicki, J. Tanori, I. Lisiecki, A. Filankembo, Adv. Mater. 11 (1999) 1358.
[17] M. Li, H. Schnablegger, S. Mann, Nature 402 (1999) 393.
[18] X. Peng, L. Manna, W. Yang, J. Wickham, E. Scher, A. Kadavanich, A.P. Alivisatos, Nature 404 (2000) 59.
[19] H. Masuda, K. Fukuda, Science 268 (1995) 1466.